Supporting Information

In situ grafting silica nanoparticles reinforced nanocomposite hydrogels

Jun Yang*, Chun-Rui Han, Jiu-Fang Duan, Feng Xu, Run-Cang Sun

College of Materials Science and Technology, Beijing Forestry University, Beijing, China

*Corresponding author: yangjun11@bjfu.edu.cn

Experimental

Large strain mechanical behavior

Loading-unloading cycles were conducted to examine the viscoelastic behavior and self-recovery capabilities. Cycles were applied from zero to a maximal nominal strain and then the sample was unloaded at the same strain rate until zero stress was achieved. The sample was then sealed in a polyethylene bag and submerged in mineral oil (35 °C) to prevent water evaporation for 2 h. After that, the specimen was deformed again until it reached the next targeted strain. The elastic recovery values of the hydrogels were obtained from these cyclic tests.

Rheological measurements

Oscillatory shear tests, corresponding to low deformation levels (0.1%), were performed with a TA AR2000 rheometer equipped with a Peltier device for temperature control, in an angular frequency range from 0.1 to 100 rad/s using 25 mm diameter parallel plates. Typically, three samples were analyzed and the repeatability of the measurements of the storage moduli and loss moduli were usually with a range of 5%.

Molecular weight detection

The dried SNP gel was cut into small pieces (～0.1 g), immersed into hydrofluoric acid solution (50 mL, 15 wt%) for 24 h under stirring at room temperature and neutralized by the addition of sodium carbonate solution (0.5 M). Then the solution was filtered through polytetrafluoroethylene membrane with a pore size of 0.45 μm and the molecular weight of graft chain was measured by size exclusion chromatography (SEC) (Tosoh Bioscience, TSK-GEL G3000SWXL 300 mm×7.8 mm). The solution was diluted to 5 mg/mL in phosphate buffer (NaH_2PO_4 0.01 mol/L and

Na_2HPO_4 0.02 mol/L, pH 7) and the degassed phosphate buffer was used as mobile phase at flow of 0.25 mL/min. Monodisperse dextran standard samples obtained from Pharmacia Biotech Corp. were used to obtain a universal calibration curve for calculating the molecular weights of the polymers herein.

FTIR measurements

Fourier transform infrared spectroscopy was performed on an infrared spectrophotometer (Nicolet iN10-MX, Thermo Scientific). The spectra were obtained in an optical range of 600 to 4000 cm^{-1} using an average of 32 scans and a resolution of 4 cm^{-1}.

Tearing test

The tearing test was conducted in Tearing Mode with a Zwick 005 at room temperature. The samples were cut into a trouser-shape with a cutting machine. The two arms of the samples were clamped, and one arm was pulled upward at a constant velocity of 30 mm/min, while another arm was fixed. The initial sample dimension *l* (length) = 100 mm, *w* (width) = 15 mm, and *h* (height) = 10 mm were fixed for the tests. The effect of initial crack length was examined with various crack lengths (*c*). The tearing energy, *T*, was calculated from work required to tear a unit area by[1]

$$T=2F/w$$

where *F*, and *w* were the average force during steady-tearing state and thickness of the sample, respectively.

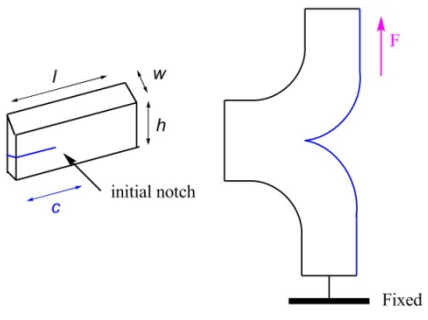

Scheme of the tearing test geometry

Results and discussion

FTIR Analysis

There appeared C=C stretching vibration peak at 1630 cm^{-1}, and C=O stretching vibration peak

at 1735 cm^{-1}, respectively (Fig.S1). The results indicated that the SNPs were modified by silane coupling agent and can be applied to anchor acrylic acid via free radical polymerization.

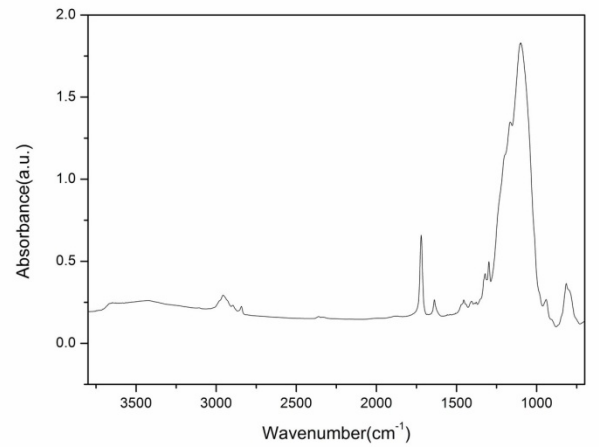

Fig.S1 FT-IR characterization of SNPs modified by silane treatment.

Gelation Process

To examine the SNP-PAA system gelation time (t_g), the rheological measurements were conducted to determine the gelation time. As indicated in Fig.S2, the values of storage moduli (G') and loss moduli (G'') as a function of frequency at three typical times were measured and there exhibited a cross-over curves at 25 min, which was considered as the gelation time. In fact, at the initial stage, the system showed pronounced viscous properties where liquid like state dominated the system ($G'<G''$), then there appeared a cross-over curve at 25 min which followed the same frequency dependence. Next, the solid like elastic features became dominately ($G'>G''$) and the appearance of sample transferred from initial solution to bulk gel.

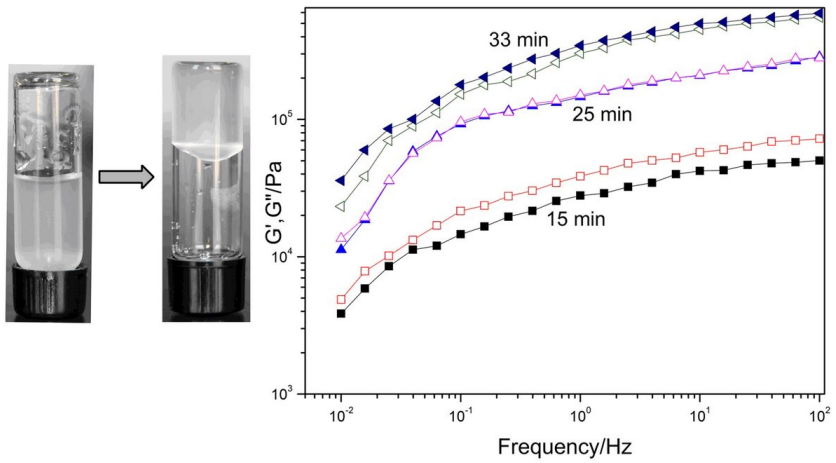

Fig.S2 Typical evolution of storage moduli G' (full symbols) and loss moduli G'' (open symbols)

as a function of frequency within the gelation process for SNP 0.1.

Constrained Polymer

The tensile measurements have indicated the SNP mechanical reinforcement role in nanoparticle clusters, which naturally encourage us to demystify the mobility of the polymer chains on the surface of SNP, termed as "glassy-like layer".[2,3] Assuming connections between clusters is generated by the immobilized polymer segments, the volume fraction of constrained is related to the height of loss factor in the frequency spectra (Fig. S3). It is known that the value of tan δ peak is proportional to the degree of freedom of molecular motion, where the polymer layer is thick and the filler-polymer interaction is strong and hard to be peeled from the matrix at a high filler loading.[4] The interpenetrated clusters can be viewed as a network where the closely stacked polymer chains in the vicinity of filler surface is similar to glassy zone and the polymer matrix is analogous to the amorphous region. Thus, the covalent bonds of PAA chains on SNP surface resulted in the shell of immobilized glassy layer and significantly enhanced the modulus of the nanocomposites.

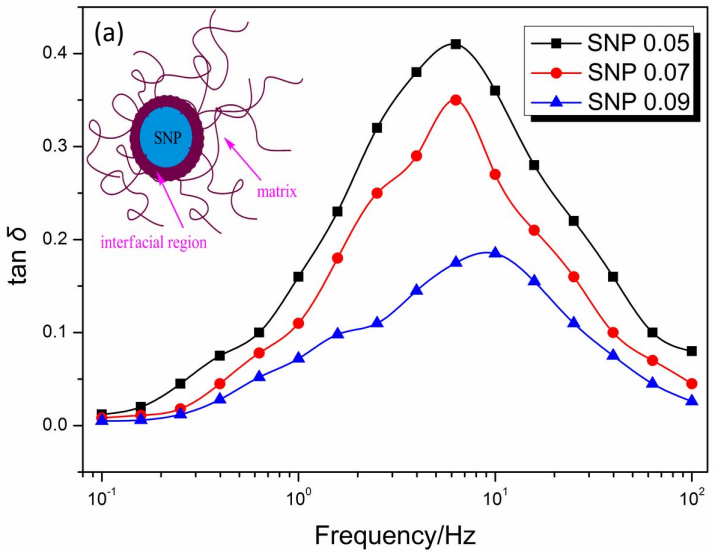

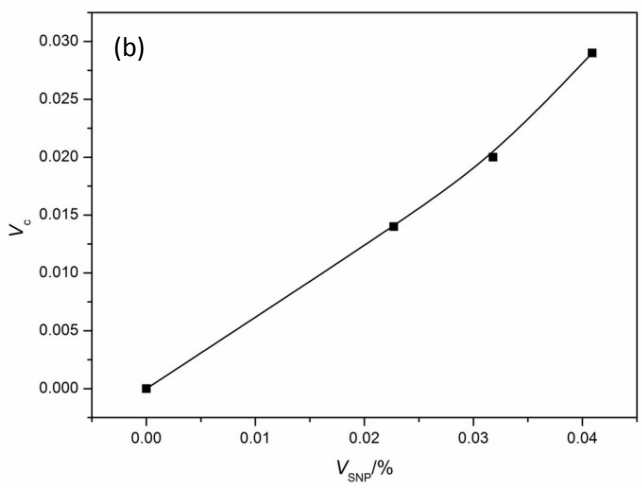

Fig.S3 (a) Representative of loss factor (tan δ) for nanocomposites at different SNP concentrations, (b) Volume of constrain polymer fraction V_c as a function of SNP volume fraction. The insert scheme in (a) illustrates the mobility of PAA chains on SNP surface with two main regions: an interfacial region near the SNP surface constrain the chain dynamic mobility, and a primary region has a mobility comparable to segments in PAA matrix with increasing distance from the SNP surface.

In principle, the height of loss factor in frequency sweep can be related to the fraction of polymer chains that participating at immobilization of polymer chains in the vicinity of filler surface.[3] Thus, the SNP reinforcement capability is related to the extensive boundary zone that is well mixed with the matrix polymer, leading to the volume fraction of constrained polymer chains to increase with increasing SNP content. Specifically, the fraction of constrain polymer volume (V_c) can be calculated by[4]

$$V_c = 1 - H/H_0(1-V_{SNP}) \qquad (1)$$

where V_{SNP} is volume fraction of loaded SNP, and H and H_0 are the height of the tan δ peak of nanocomposite and pristine polymer, respectively (assuming $V_c = 0$ for amorphous phase in pristine PAA matrix and density of SNP of 2.2 g/cm^3). The values of are present in Fig.S3(b), where the increase of SNP content led to more constrained polymer chains and contributed to significantly mechanical reinforcement.

Molecular Weight Measurements

The reaction time φ dependency of molecular weight (M_w) of SNP surface grafted polymer

chains (φ=(t-t_g)/t, where t was the measurement time, t_g was the gelation onset time, φ and was the relative distance from the gel point) was illustrated in Fig. S4. One can note that the curve can be divided into three stages: at the early stage of pregel region (φ<0), the value of M_w increased steeply from 70 to 2,100 Da. Then there exhibited a sudden change around the gelation point (φ=0) where M_w increased to 7,550 Da, and the curve gradually leveled off as the system attained the postgel stage. This trend could be explained that at the initial stage, the monomer began to graft on the SNP surface and form free-moving SNP-PAA clusters. As the reaction progressed, the length of polymer chains on SNP surface increased and became relative compact cluster near the t_g, which corresponded to a higher conversion ratio. Then there exhibited some sudden increase at the time of t_g, the length of grafted chains reached more than half of the distance between two neighboring SNPs and the grafted polymer chains became entangled, where these clusters interconnected to form a continuous network. With the gelation further proceeded, the increase of M_w became relative level-off, implying a post mature cross-linked network stage.

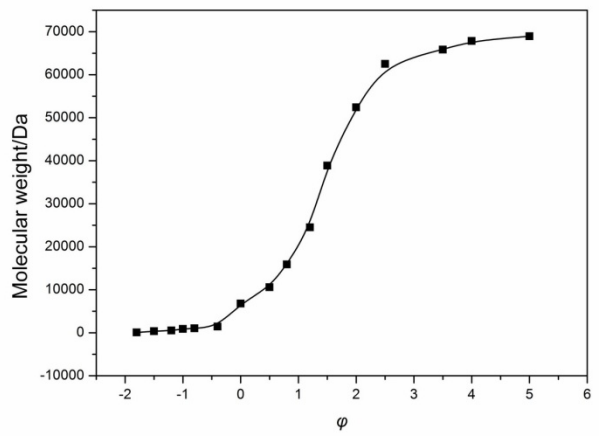

Fig.S4 Molecular weight of grafted polymer chains at different stages for SNP 0.1.

Elastic Properties

For SNP-PAA systems, the gelation depended on the formation of three dimensional percolation lattice model, implying the growth and interconnection of aggregates until the whole volume was percolated and attained an infinitely large network. The storage moduli (G') reflecting the strength features of the gels was illustrated in Fig.S5, which could be divided into three regions by the SNP concentration (C_{SNP}). (1) In the C_{SNP} less than macroscopic percolation transition region, the polymer-rich phase transformed into isolated SNP-PAA clusters and the strength of the systems

was weak. (2) When the C_{SNP} was close to the critical value, the phase separation of initial stage dominated the network formation and the mechanical properties of gels. That is, above this critical value, the system exhibited phase separation phenomenon from initial homogeneous phase (sol) with free-moving nanoparticles to the aggregation of those nanoparticles entrapped phase (gel). (3) As the C_{SNP} continually increased, the influence of phase separation on SNP-PAA systems would be weakened due to the chain overlapping effect, and the significant reinforcement effect was observed, i.e., the filler strong interactions were ascribed to the existence of a filler network spanning the whole range of polymer matrix. Due to some individual polymer chains may simultaneously adsorbed to different SNPs via hydrogen bonding and thus adopt stretched configurations, these nanosized particles could be connected by polymer chains even their distance was much longer than their size.

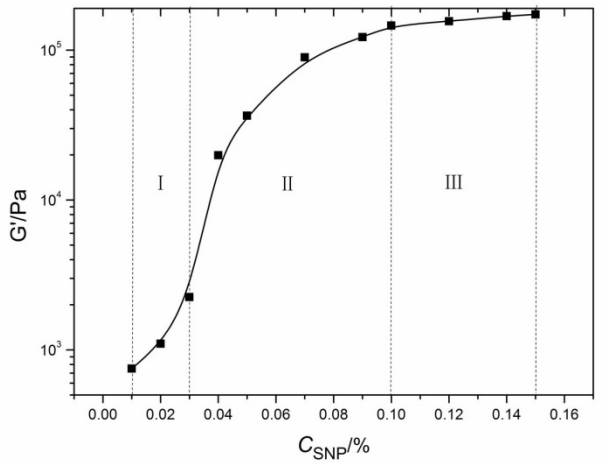

Fig.S5 Storage moduli of SNP gels as a function of C_{SNP} at a frequency of 0.1 Hz.

Loading-unloading Cycle

The feature of the sacrificial bonds (dynamic entanglements) in the nanocomposites, hysteresis, was examined by the cyclic loading-unloading measurements, and the tensile stress versus strain curves for the SNP gels were shown in Fig.S6 (a)&(b). The high modulus was attributed to the multifunctional cross-link character of the SNPs, and the high elongation and strength was due to the ability of the physical interactions between clusters to dissipate energy. It is known that for a chemically cross-linked gel, almost no hysteresis loop would appear and dissipation of the matrix is negligible.[6] In contrast, the SNP gels showed notable hysteresis by loading-unloading curves, implying a form of network change during deformation. It was speculated that these polymer

chains on SNPs surface in coiled conformation started to be extensively elongated and this process could dissipate a huge amount of energy and increase the resistance against crack propagation. Thus, the addition of SNPs to the matrix induced the viscoelastic properties and increased toughness. Furthermore, the SNP induced dissipative capability was time dependent in repeated loadings, a relevant indicator of internal self-healing capabilities (Fig.6(c)). In the second and more cycles of loading-unloading measurements, the gel was weaker than the first loading and the extent of recovery decreased with the number of cycles, indicating internal damage was partial healed by storing the gels for some time before reloading.

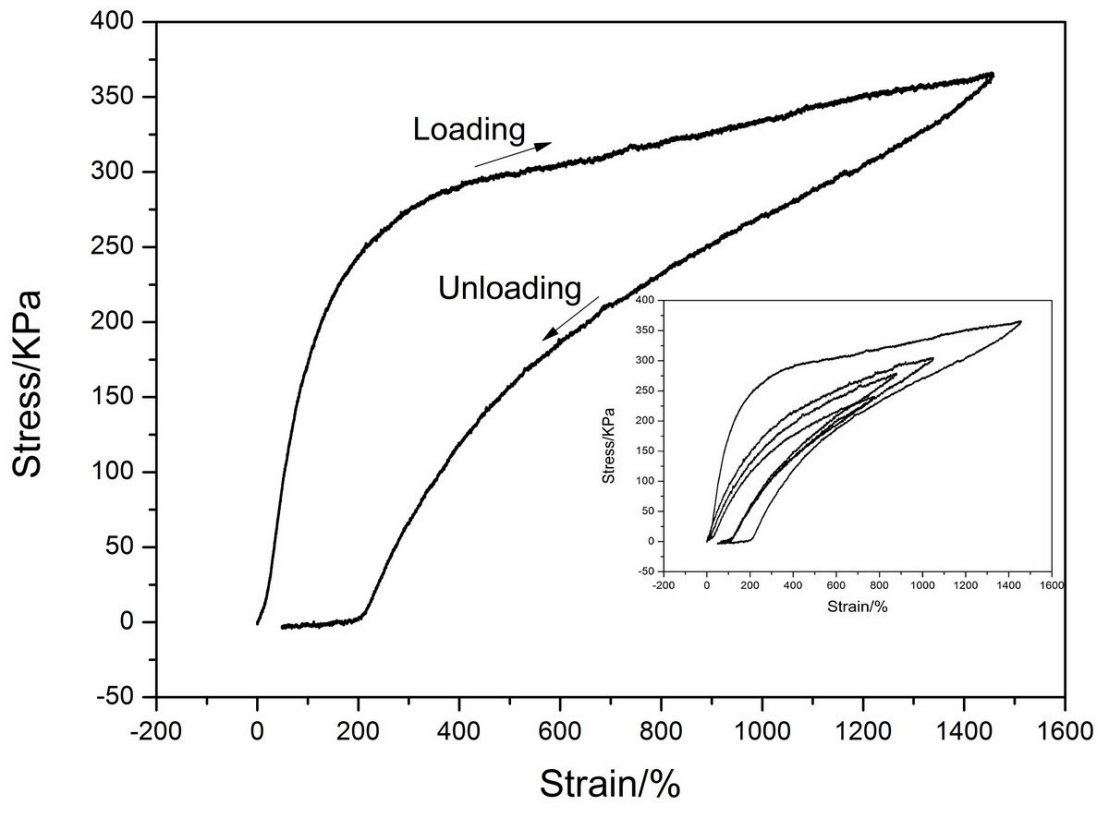

(a)

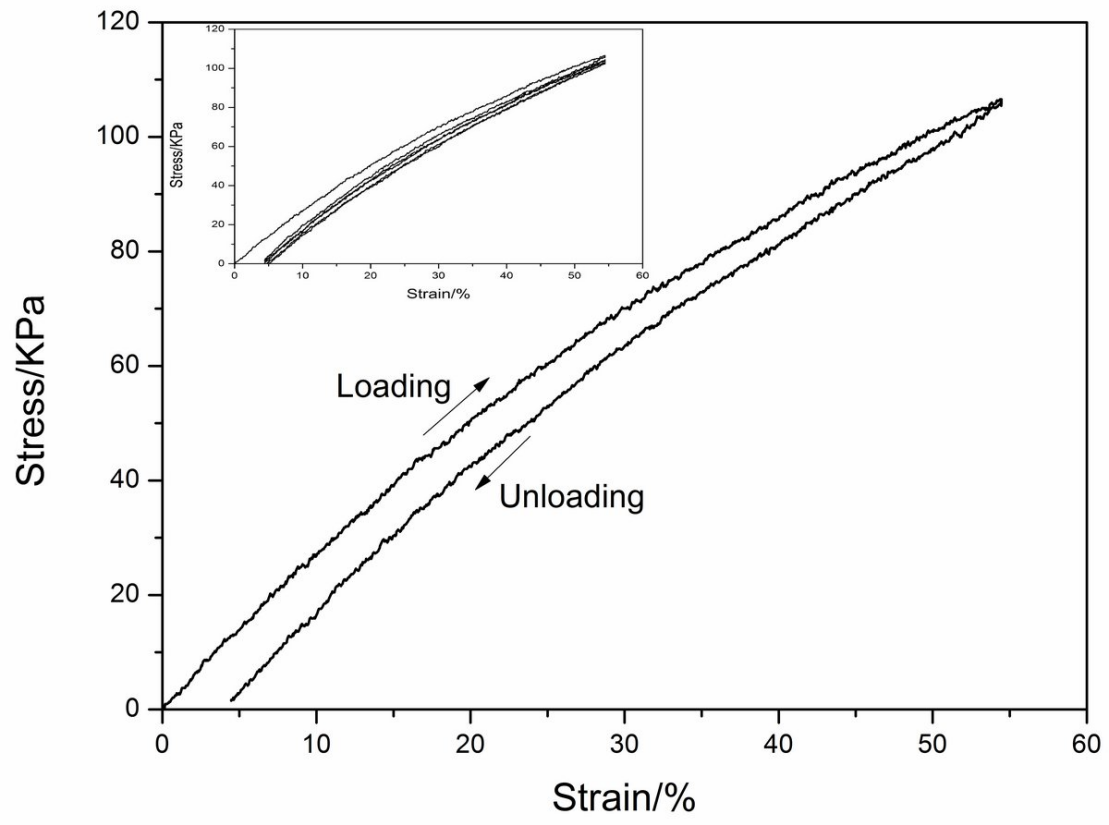

(b)

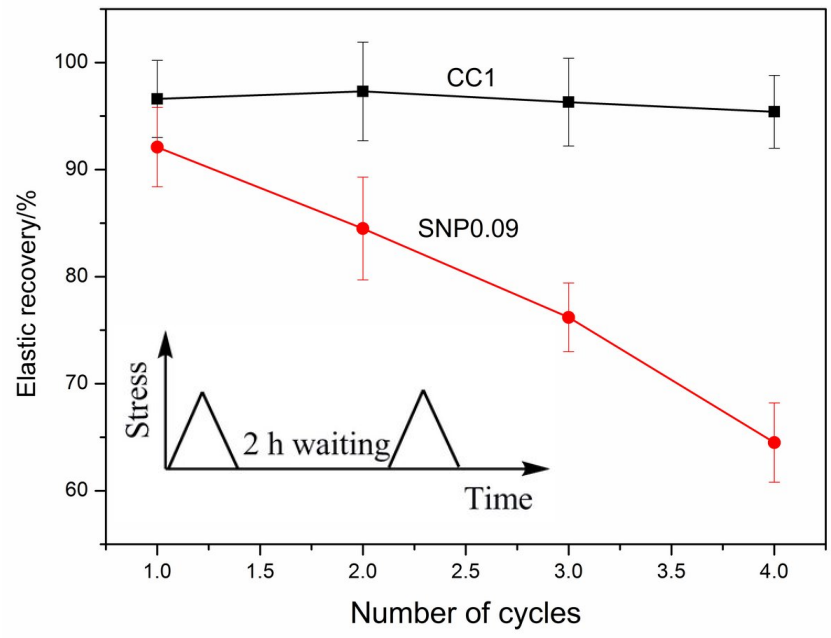

(c)

Fig.S6 Curves of consecutive loading-unloading cycles of SNP 0.09 (a), CC1 (b) and their recovery as a function of the number of cycles (c).

Tearing Tests

When a nanocomposite hydrogel having an initial notch is stretched perpendicular to the crack direction, a blunting with a trumpet shape occurs which avoids the stress concentration at all in front of the crack tip.[7] For example, the tearing energy did not vary much by initial lengths in the range of $c/l < 0.3$, then the fracture energy decreased to less than 20% of its value when the ligament length reached more than 40% of the whole sample length (Fig.S7). Whereas for the pristine PAA counterparts (CC 1), the fracture energy remained at a low value once the samples were notched, suggesting the crack fast propagated even at a small crack due to the lack of mobile nature of SNP/PAA clusters at the crack tip.

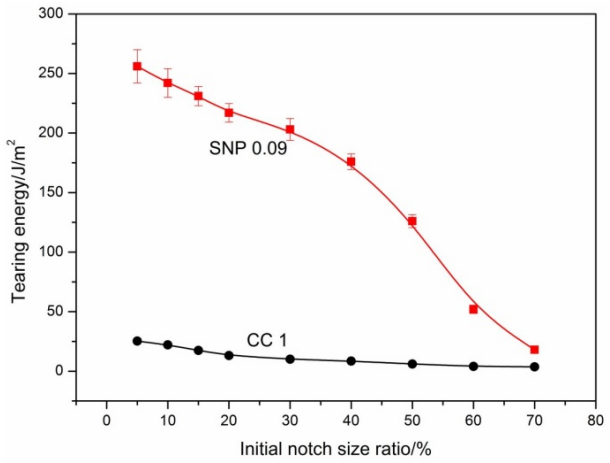

Fig.S7 Effect of initial notch size ratio (c/l) on tearing energy for SNP 0.09.

In fact, when a notched gel is stretched, the stress distribution is inhomogeneous and the polymer segments directly ahead of the crack are stretched more than the chains elsewhere. In the case of chemically cross-linked PAA systems, only the polymer chains ahead of the notch need to unzip and the notch in the network turns into a running crack fast, leading to the energy dissipates over a localized domains. In sharp contrast, in SNP/PAA nanocomposite hydrogels, the number of chains that participate in energy-dissipating process is increased (Fig.S8). Before the chains ahead of the notch required to be broken, the hybrid network unzips over a large region around the notch, providing efficient energy transfer between the directly coupled two components.[5]

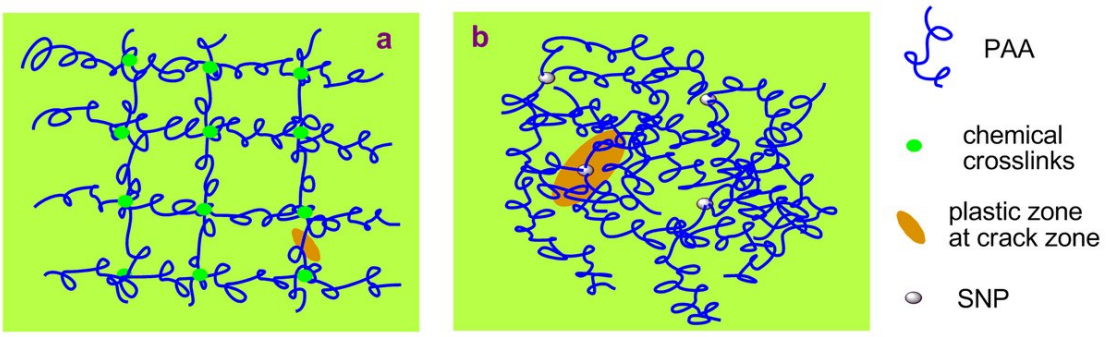

Fig.S8 Schematic showing hydrogels energy dissipation mechanism. (a) In the chemically cross-linked PAA gels, those chains crossing the crack plane need to break and chains elsewhere remain intact. (b) In the SNP/PAA hybrids, the multi-functional SNPs are bridged by the grafted chains and stabilize deformation. The silane interactions between two components transfer the stress over a large zone, and noncovalent entanglements serve as sacrificial bonds provide viscoelastic deformation over this large zone around the root of the notch.

References

(1) R. G. Stacer, E. D. Von Meerwall and F. N. Kelley, *Rubber Chem. Technol.* 1985, **58**, 913-923.

(2) D. Shah, P. Maiti, D.D. Jiang, C.A. Batt and E.Giannelis, *Adv. Mater.* 2005, **17**, 525-528.

(3) N. Jouault, P. Vallat, F. Dalmas, S. Said, J. Jestin and F. Boué, *Macromolecules* 2009, **42**, 2031-2040.

(4) Y. Kojima, A. Usuki, M. Kawasumi, A. Okada, Y. Fukushima, T. Kurauchi and O. Kamigaito, *J. Mater.Res.* 1993, **8**, 1185 – 1189.

(5) M. A. Haque, T. Kurokawa, G. Kamita and J. P. Gong. *Macromolecules* 2011, **44**, 8916–8924.

(6)L. R. G. Treloar, The Physics of Rubber Elasticity. Oxford University Press, 1975.

(7) E.E. Gdoutos, Fracture Mechanics – An Introduction. Kluwer Academic Publishers, Dordrecht, The Netherlands, 1993.